

1 **A vertical transport window of water vapor in the troposphere**  
2 **over the Tibetan Plateau with implication for global climate**  
3 **change**

4  
5 **Xiangde Xu<sup>1,2</sup>, Chan Sun<sup>1,2</sup>, Deliang Chen<sup>3</sup>, Tianliang Zhao<sup>1\*</sup>, Jianjun Xu<sup>4</sup>,**  
6 **Shengjun Zhang<sup>2</sup>, Juan Li<sup>1</sup>, Bin Chen<sup>2</sup>, Yang Zhao<sup>2</sup>, Hongxiong Xu<sup>2</sup>, Lili Dong<sup>2</sup>,**  
7 **Xiaoyun Sun<sup>1</sup>, Yan Zhu<sup>1</sup>**

8  
9 <sup>1</sup> Nanjing University of Information Science and Technology, Nanjing 210044, China;

10 <sup>2</sup> State Key Laboratory of Disastrous Weather, China Academy of Meteorological  
11 Sciences, Beijing, 100081, China;

12 <sup>3</sup> Regional Climate Group, Department of Earth Sciences, University of Gothenburg,  
13 Sweden;

14 <sup>4</sup> South China Sea Institute of Marine Meteorology, Guangdong Ocean University,  
15 Zhanjiang 524088, China

16 \* Corresponding author. **Email:** [tlzhao@nuist.edu.cn](mailto:tlzhao@nuist.edu.cn)

21 **Abstract**

22 By using the multi-source data of meteorology over recent decades, this study  
23 discovered a summertime “hollow wet pool” in the troposphere with a center of high  
24 water vapor over Asian water tower (AWT) on the Tibetan Plateau (TP), which is  
25 featured by a vertical transport “window” in the troposphere. The water vapor transport in  
26 the upper troposphere extends from the vertical transport window over the TP with the  
27 significant connections among the Arctic, Antarctic and TP regions, highlighting the  
28 effect of TP’s vertical transport window of water vapor in the troposphere on global  
29 change of water vapor. The vertical transport window is built by the AWT’s thermal  
30 forcing in association with the dynamic effect of the TP’s “hollow heat island”. Our study  
31 improves the understanding on the vapor transport over the TP with an important  
32 implication to global climate change.

33

34

## 35 **1. Introduction**

36 The Tibetan Plateau (TP) is the largest high terrain in the world, known as "the roof  
37 of the world" with an averaged altitude over 4,000 meters. The rivers, such as the  
38 Yangtze River, Yellow River, Lancang River and Ganges River, are all originated from  
39 the TP, which is regarded as the "Asian Water Tower" (AWT) (Xu et al., 2008). The  
40 three-river-source (Yangtze, Yellow, and Lancang Rivers) region (TRSR) in the eastern  
41 TP is the core area of the AWT over the plateau (Xu et al., 2014). The observed "CISK-  
42 like mechanism" is an important mechanism sustaining the atmospheric "water tower"  
43 over the AWT (Xu et al., 2014). Connecting with the cloud and precipitation in the AWT,  
44 the plausible hydrological cycles could be realized with the transport of water vapor from  
45 tropical oceans up to the TP (Xu et al., 2014).

46

47 Water vapor plays an important role in global environment and climate changes  
48 (Tian et al.,2009; Solomon et al.,2010). The ratio of strong convective clouds to total  
49 clouds over the Tibetan Plateau (TP) is about 5 times to the global ratio, and the frequent  
50 occurrences of strong convective clouds could be largely attributed to the TP's large  
51 topography (Luo et al.,2011; Su et al.,2006). The water vapor in the upper troposphere is  
52 mainly originated from the tropical lower troposphere through vertical transport and  
53 evaporation of convectively transported or in situ produced cloud ices (Tian et al.,2004;  
54 James, et al.,2008). Water vapor was first lifted by convection over the Bay of Bengal  
55 and the South China Sea and then transported upwards the tropical tropopause layer via  
56 the monsoon anticyclonic circulations towards Northwest India (Yanai, et al., 1973; Chen,

57 et al., 2012). TP is a moisture sink in summer, having a net moisture convergence of 4  
58 mm each day, where the convergences were enhanced from 1979 to 2018 (Feng and  
59 Zhou, 2012; Xu, et al., 2020). In general, Asian monsoon circulation provides an  
60 effective pathway for regional water vapor transport to the TP (Wang, et al.,2017). An  
61 important role of the anticyclone over the TP is verified in the exchange of water vapor  
62 between the troposphere and stratosphere (Garny, et al., 2016; Fu, et al., 2006) . Many  
63 studies have been focused on the transport of water vapor into upper troposphere and  
64 lower stratosphere from the tropical oceans to the high-altitude TP (Chen, et al., 2012;  
65 Wang, et al.,2017; Xie, et al.,2018; Randel, et al.,2013). However, inadequate attention  
66 has been paid to the vertical transport of water vapor in the troposphere over the TP,  
67 especially in respect of the underlying mechanism and the consequences on global  
68 climate.

69

70 The following questions are of great concern in the TP' vertical transport of water  
71 vapor study with the implication for global change, for example, what is the formation  
72 mechanism on the vertical transport window of water vapor in the troposphere on the TP?  
73 How is the vertical transport of water vapor in the troposphere constructed with the  
74 special column of apparent heat source in the AWT over the TP ? How is the global  
75 effect of the vertical transport window of water vapor in the troposphere on the TP? From  
76 the perspective of global atmospheric energy and water vapor exchanges, this study  
77 characterizes a window of water vapor vertical transport within the troposphere over the  
78 TP and the implication for global change.

79

80 **2. Data and Methods**

81 The daily meteorological data of cloud amount are provided by the meteorological  
82 observatories in the TP in the period of 1979 to 2018. The AIRS remote sensing products  
83 of water vapor from 2003 to 2018 and the ECMWF-interim data of meteorology from  
84 1979 to 2018 are used in this study.

85

86 In this study, the inverse algorithm is used to calculate the apparent heat source  $Q_1$ ,  
87 and the formula is as follows ( Su et al.,2006) :

88 
$$Q_1 = C_p \left[ \frac{\partial T}{\partial t} + \vec{V} \cdot \nabla T + \left( \frac{p}{p_0} \right)^k \bar{\omega} \frac{\partial \theta}{\partial p} \right] \quad (1)$$

89 where  $T$  is the air temperature;  $\omega$  is the vertical velocity at the  $p$  coordinate,  
90  $P_0 = 1000$  hPa;  $k = R/C_p$  ;  $V$  is the horizontal wind vector;  $\theta$  is the potential temperature.

91 Vertical integration of  $Q_1$  is expressed as:

92 
$$\langle Q_1 \rangle = \frac{1}{g} \int_{p_t}^{p_s} Q_1 dp \quad (2)$$

93 where  $p_s$  is the surface air pressure, and  $p_t$  is the top air pressure, here taken as 300hPa.

94

95 In order to analyze the relationship between water vapor sources and vapor  
96 transport channels in the atmospheric water cycle, the correlation vector calculation was  
97 used to calculate the temporal and spatial variations of the water vapor transport channels.  
98 The expression is:

99 
$$\vec{R}(x, y) = R_u(x, y)i + R_v(x, y)j \quad (3)$$

100 where  $\vec{R}(x, y)$  represents the correlation vector in which  $R_u(x, y)$  represents the  
101 correlation coefficients between water vapor and the component of latitudinal water  
102 vapor flux  $qu$ , and  $R_v(x, y)$  represents correlation coefficients between water vapor and  
103 longitudinal water vapor flux components  $qv$ .

104

### 105 **3. Results and discussion**

#### 106 **3.1 The structures of vertical transport window of water vapor over the TP**

107 With the use of satellite remote sensing products from 2003 to 2016, the global  
108 distribution of the total water vapor from 500hPa to 300hPa in the troposphere was  
109 shown in Figure 1a . The results indicate that there is a high value center of water vapor  
110 in the mid- and upper troposphere over the TP, extending southwards to the Bay of  
111 Bengal, India and Northern Southeast Asia. It is worth noting that the fraction of strong  
112 convective clouds to the total cloud ranges from 4.0 % to 21.0 % in the TP, and during the  
113 summer season the thermal forcing of TP is dominated by the latent heat released by  
114 cloud and precipitation (Fu et al.,2006; Dessler et al.,2006; Gao et al.,2014). The intense  
115 mesoscale convective activity, which is represented with the low cloud fraction based on  
116 the cloud characteristics observed in the TP, and the "massive chimney effect" of huge  
117 cumulonimbus cloud drive the transport of atmospheric heat and water vapor to the upper  
118 troposphere (Fu et al.,2006; Xie et al.,2018). Based on Chinese Third Tibetan Plateau  
119 Experiment-Observation of Boundary Layer and Troposphere (2014–2017), it is observed  
120 in the TP that the cloud-top height was averaged around 11.5 km (a.s.l.) with its

121 maximum value exceeding 19 km (a.s.l.) , and the mean cloud-base height at 6.88 km  
122 (a.s.l.) during the observation period, reflecting the TP's deep convection in the  
123 troposphere and its impact on the upper troposphere.

124

### 125 **3.2 Global effect of the vertical transport window over the TP**

126 The vertical section of the correlation coefficients along the south-north direction  
127 between the low cloud cover on the TP and the global water vapor are presented in Figure  
128 1b. The obviously upward movement of water vapor over the TP can be seen in Figures  
129 2a. It could be noticed that there exist the structures similar with the massive chimney  
130 between the convective cloud and the water vapor on the TP (Figures 1b and 2a). Figures  
131 2b and 2c show significant correlation between convective clouds over the AWT and the  
132 changes of global water vapor from 1979 to 2018. Significant correlations extend from  
133 the TP southward and northward in the upper troposphere. It is remarkable that the high  
134 correlation areas passing the 90% confidence level expand towards the polar regions of  
135 both the southern and the northern hemispheres (Figures 1b, 2b and 2c), depicting the  
136 relation between the convective clouds and the global water vapor in the upper  
137 troposphere across the northern and southern hemispheres for an implication of the TP to  
138 global climate change.

139 The distributions of high positive correlation coefficients between low cloud  
140 cover over the TP and the global water vapor in the upper troposphere are calculated by  
141 ECMWF-interim reanalysis data (Figure 3a). It can be found that there is a region with  
142 highest values of correlation coefficients in the upper troposphere (500hPa-300hPa),  
143 covering a banded large area from the plateau across the lower latitude tropical zone to

144 the polar regions, indicating the significant correlations between convective cloud  
145 activities on the TP and the global water vapor in the upper troposphere, especially in the  
146 polar region of the southern hemisphere area (Figure 3a), which could be reflected an  
147 importance of the thermal forcing of TP in global changes of water vapor.

148 The strong anticyclone in the upper troposphere over the southeastern TP takes a  
149 significant part in the upward transport of water vapor in the troposphere and stratosphere  
150 (Garny, et al., 2016; Fu, et al., 2006). In order to understand the effect of the vertical  
151 transport window of troposphere over the TP on the global water vapor distribution from  
152 the perspective of the dynamic effect of anticyclone over the plateau driven by the heat  
153 sources, we presented the distributions of correlation coefficients between daily mean  $Q_1$   
154 in the TP and global water vapor flux in July from 2014 to 2016 at 300hPa (Figure 3b.)  
155 Driven by the heat source of the TP, the anticyclone is formed in the upper troposphere  
156 over the TP and surrounding regions, which governed the water vapor transport from the  
157 TP not only to the surrounding area, but also extending to the north and south poles along  
158 the long-range transport channels (Figure 3b), which indicates the vertical transport  
159 window effect of the TP on global water vapor transport, especially over high-latitude  
160 regions such as the Arctic and Antarctic. To further verify the global transport pathways  
161 of water vapor from the TP, we used the methods of composite analysis to characterize  
162 global distribution of water vapor transport fluxes at the 300hpa in the years to  
163 anomalously high and low  $Q_1$  over the TP. The TP's anticyclone in the upper troposphere  
164 is often associated with deep convection in the troposphere (Garny, et al., 2016). Figure  
165 3c shows that in years with higher  $Q_1$ , stronger anticyclone formed at the upper  
166 troposphere (Figure 3b), which maintains the upward transport of water vapor to the

167 upper troposphere, with strong transport of water vapor transport the arctic and antarctic  
168 (Figure 3c), confirming the impact of the vertical transport in the troposphere driven by  
169 heat released within AWT in the TP on global water vapor transport especially to the  
170 polar regions.

171 The Indian continent heats up from spring to summer, hence the convection draws  
172 moisture northwards from the Bay of Bengal, Arabian Sea and Indian Ocean, leading to  
173 precipitation in the Himalayas and beyond (Yanai et al., 1973). In Figure 3d, it could be  
174 found that, driven by the strong apparent heat source, the water vapor flows from the low  
175 latitude ocean could build a remarkable channel to the TP. The key entrance to the water  
176 vapor passage is just the intersection of the Himalayas on the southern slope of the TP.  
177 This region constitutes a special canyon pass in the plateau with deep valleys, making a  
178 perfect entrance zone for the oceanic warm-wet water flows (see the terrain distribution  
179 inserted in the lower right corner of Figure 3d).

180 FLEXPART trajectory model (Stohl, et al., 2005; Reale, et al 2001; James, et al,  
181 2004) was used to simulate the spatial and temporal changes of water vapor transport to  
182 the TRSR over the TP, driven with the ERA-Interim reanalysis data of meteorology with  
183 horizontal resolution of  $0.75^{\circ} \times 0.75^{\circ}$  in July 2009. In the FLEXPART particle diffusion  
184 model, the 80000 particles was released at the TRSR ( $90^{\circ}$ - $102^{\circ}$ E and  $30^{\circ}$ - $35^{\circ}$ N). In Figure  
185 3f, it can be found that the water vapor in the TRSR was traced to water vapor source on  
186 the tropical Indian Ocean. The water vapor from the central Indian Ocean in the southern  
187 hemisphere can be transported along the Somali jet flow through the Arabian Sea to the  
188 TP. The water vapor from the South China Sea and the Bay of Bengal was transported to

189 the TP converging over the TRSR (Figure 3f), characterizing the water vapor transport  
190 channel from the southern hemispheric and low latitude oceans to the TP.

191 According to the correlation analysis of water vapor transport, the water vapor  
192 source of the AWT can also be traced back to the ocean surface water vapor source  
193 region with water vapor positive correlation extreme value region in the Chagos  
194 Archipelago of the Central Indian Ocean near 10°S south of the equator (Figure 3e),  
195 revealing that the TP is the confluence area of the hemispherical water vapor from the  
196 southern Indian Ocean.

197

### 198 **3.3 The transport window of water vapor driven by the AWT**

199 Through the correlation analysis of the column apparent heat  $Q_1$  over the TP as  
200 well as the three-dimensional structure of vorticity and divergence, it can be found that  
201 the apparent heat source  $Q_1$  in the TP is an important forcing factor (Figure 4). The  
202 results show that the air heat island in the AWT is located at 300-500 hPa in the upper  
203 troposphere, which is regarded as the high apparent heat  $Q_1$  area significantly related to  
204 the convective clouds and the strong ascending movement (Figures 4a and 4d). Figures  
205 4b,4c, 4e and ff present the correlations of the column apparent heat  $Q_1$  in AWT with the  
206 divergence and vorticity fields over the TP, which can describe the effective "suction  
207 effect" with divergence (negative vorticity) at upper levels and convergence (positive  
208 vorticity) at lower levels in the troposphere. The  $Q_1$  is significantly released in the  
209 convective clouds and the strong ascending movement, and there exists a strong  
210 anticyclonic circulation in the upper troposphere over the region of the AWT in the  
211 southeast of the plateau (Figure 3b). In addition, the lower troposphere is the center of

212 strong convergence and strong vorticity. Figure 3g shows the difference of vapor  
213 transport flux and specific humidity at 500hPa in summer between anomalously high and  
214 low  $Q_1$ . When the  $Q_1$  in TRSR is anomalously high, large water vapor from the tropical  
215 oceans is transported across the Bay of Bengal and the Indian peninsula, and entered the  
216 TP from the southern edge, revealing the TP's thermal effect could make a strong vapor  
217 transport channel connecting the water vapor source in the low latitude tropical oceans.

218

219 All these results reveal the effective "pumping effect" of the vertical configuration  
220 with low-level cyclonic circulation and high-level divergence with anticyclone  
221 circulation over the TP. The strong confluence effect building the vertical transport  
222 window of water vapor could be driven by the elevated heating on the TP in the  
223 troposphere with the water vapor flow, making a strong vapor transport connecting the  
224 water vapor source in the low latitude oceans with the high water vapor center over the  
225 core area of AWT over the TP. The water vapor transport connect from the vertical  
226 transport window over the TP and the Arctic, Antarctic regions in the upper troposphere,  
227 highlighting the effect of TP "hollow wet pool" on global climate change.

228

#### 229 **4. Conclusion**

230 By using the multi-source data of meteorology over recent decades, this study  
231 discovered a summertime "hollow wet pool" in the troposphere with a center of high  
232 water vapor over AWT on the highly elevated TP, which is featured by a vertical  
233 transport window with the transport flux of water vapor in the troposphere. Driven by the

234 strong TP's heat source, water vapor flows connect the AWT over the TP with the low-  
235 latitude oceans. Significant correlations exist between convective activities on the TP and  
236 global water vapor in the upper troposphere,. The water vapor transport from the TP's  
237 vertical window in the upper troposphere extends from the TP globally towards the  
238 northern and southern hemispheres with the significant connections among the three  
239 poles of Arctic, Antarctic and TP regions, highlighting the effect of TP's vertical  
240 transport window of water vapor on global climate change. The vertical transport window  
241 is built by the AWT's thermal forcing in association with the dynamic effect of the TP's  
242 "hollow heat island" as well as the effective "pumping effect" on vertical transport with  
243 low-level convergences with cyclonic circulation and upper-level divergences with  
244 anticyclone circulation in the troposphere over the TP.

245 Basd on this observational study, a conceptual model of the comprehensive relation  
246 of the TP region with the global energy and water cycles is put forward for the vertical  
247 transport window of vapor in the troposphere driven by the thermal forcing in the core  
248 region of the AWT over the TP (Figure 5), where the water vapor source is traced back to  
249 tropical ocenas and the Southern Hemisphere. The thermal effect of the TP could sustain  
250 the vertical upward transport of the energy and water vapor. The water cycle in the AWT  
251 clearly displays the linkages of the vertical transport window of water vapor in the  
252 troposphere over the TP with the vapor source in the tropical oceans and the southern  
253 Indian Ocean in the lower troposphere and with the Arctic and Antarctic regions in the  
254 upper troposphere (Figure 5). Our study depicts a comprehensive understanding on the  
255 vertical water vapor transport in the atmosphere over the TP with an important  
256 implication to global climate change.

257

258 ***Data availability***

259 ERA-Interim of ECMWF (<https://apps.ecmwf.int/datasets/data/interim-full->  
260 [moda/levtype=pl/](https://apps.ecmwf.int/datasets/data/interim-full-moda/levtype=pl/)) reanalysis daily and monthly data are part of the European Center for  
261 Medium-range Weather Forecasts. AIRS Science Team/Joao Teixeira (2013), AIRS/Aqua  
262 L3 Daily Standard Physical Retrieval (AIRS-only) 1 degree x 1 degree V006, Greenbelt,  
263 MD, USA, Goddard Earth Sciences Data and Information Services Center (GES DISC),  
264 Accessed: [Jan. 2019], 10.5067/Aqua/AIRS/DATA303. The low cloud data used in this  
265 study are derived from the Data Sets of Surface Meteorological Elements in China  
266 released by the National Meteorology Information Center, China Meteorological  
267 Administration, which can be found at  
268 <https://zenodo.org/record/5121157#.YPkRHqjitPY>.

269

270 **Author Contributions**

271 Xiangde Xu, Chan Sun and Tianliang Zhao conducted the study design. Deliang Chen,  
272 Jianjun Xu and Shengjun Zhang analysed the observational data. Juan Li, Bin Chen,  
273 Yang Zhao, Hongxiong Xu, Lili Dong, Xiaoyun Sun, and Yan Zhu assisted with data  
274 processing. Xiangde Xu, Chan Sun and Tianliang Zhao wrote and revised the manuscript.  
275 Xiangde Xu, Chan Sun, Tianliang Zhao, and Jianjun Xu were involved in the scientific  
276 interpretation and discussion. All authors provided commentary on the paper.

277

278

279 **Acknowledgments**

280 This study was supported by The Second Tibetan Plateau Scientific Expedition and  
281 Research (STEP) program (2019QZKK0105) and the Scientific and Technological  
282 Development Funds from Chinese Academy of Meteorological Sciences (2021KJ022 and  
283 2021KJ013).

284

285 **Financial support.**

286 This study was supported by The Second Tibetan Plateau Scientific Expedition and  
287 Research (STEP) program (2019QZKK0105) and the Scientific and Technological  
288 Development Funds from Chinese Academy of Meteorological Sciences (2021KJ022 and  
289 2021KJ013).

290

291 **Conflict of interest**

292 *Xiangde Xu, Chan Sun, Deliang Chen, Tianliang Zhao, Jianjun Xu, Shengjun Zhang, Juan*  
293 *Li, Bin Chen, Yang Zhao, Hongxiong Xu, Lili Dong, Xiaoyun Sun and Yan Zhu declare*  
294 *that they have no conflict of interest.*

295

296

297 **References**

298 Chen, B., Xu, X. D., Yang, S., and Zhao, T. L.(2012). Climatological perspectives of air transport from  
299 atmospheric boundary layer to tropopause layer over Asian monsoon regions during boreal summer  
300 inferred from Lagrangian approach. *Atmos. Chem. Phys.* ; 12: 5827-5839. [https://doi.org/10.5194/acp-](https://doi.org/10.5194/acp-12-5827-2012)  
301 12-5827-2012

302 Dessler, A and Sherwood, S. (2004). Effect of convection on the summertime extratropical lower  
303 stratosphere. *J. Geophys. Res.* 109: D23301. <https://doi.org/10.1029/2004JD005209>

304 Feng, L., and Zhou,T. (2012).Water vapor transport for summer precipitation over the Tibetan  
305 Plateau:Multidata set analysis, *J. Geophys. Res.*, 117, D20114, doi:10.1029/2011JD017012

306 Fu, R., Hu, Y., Wright, J., Jiang,J., H., Dickinson, R., E., Chen, M., X., Filipiak, M., Read, W., G., Waters,  
307 W., W.,and Wu, D., L. (2006). Short circuit of water vapor and polluted air to the global stratosphere  
308 by convective transport over the Tibetan Plateau, *Proceedings of the National Academy of Sciences of*  
309 *the United States of America.* 103: 5664-5669. <https://doi.org/10.1073/pnas.0601584103>

310 Gao, Y, Cuo, L and Zhang, Y. (2014).Changes in Moisture Flux over the Tibetan Plateau during 1979–  
311 2011 and Possible Mechanisms. *J. Climate* ; 27: 1876-1893.[https://doi.org/10.1175/JCLI-D-13-](https://doi.org/10.1175/JCLI-D-13-00321.1)  
312 00321.1

313 Garny, H. and Randel, W. J. Transport pathways from the Asian monsoon anticyclone to the stratosphere,  
314 *Atmos. Chem. Phys.* (2016); 16: 2703–2718, [https://doi.org/10.5194/acp-16-2703-](https://doi.org/10.5194/acp-16-2703-2016) 2016,.

315 James, R. , Bonazzola, M. , Legras, B. , Surbled, K. , & Fueglistaler, S. . (2008).Water vapor transport and  
316 dehydration above convective outflow during Asian monsoon. *Geophys. Res. Lett.* ; 35:  
317 L20810.<https://doi.org/10.1029/2008GL035441>

318 James, P., Stohl, A., Spichtinger, N.: Climatological aspects of the extreme European rainfall of August  
319 2002 and a trajectory method for estimating the associated evaporative source regions. *Nat Hazards*  
320 *Earth Syst Sci*, 2004, 4, 733 – 746.

321

322 Luo, Y. , Zhang, R. , Qian, W. , Luo, Z. , and Hu, X. . (2011). Intercomparison of deep convection over the  
323 tibetan plateau--asian monsoon region and subtropical north america in boreal summer using  
324 cloudsat/calipso data. *Journal of Climate*. 24: 2164-2177.

325 Randel, W. J. & Jensen, E. J. (2013).Physical processes in the tropical tropopause layer and their roles in a  
326 changing climate. *Nat. Geosci*,6, 169. <https://doi.org/10.1038/ngeo1733>

327 Reale, O., Feudale, L., Turato, B.: Evaporative moisture sources during a sequence of floods in the  
328 Mediter-ranean region. *Geophys Res Lett*, 2001, 28, 2085 – 2088.

329 Solomon, S., Rosenlof, K. H., Portmann, R. W., Daniel, J. S.,Davis, S. M. , Sanford, T. J. and Plattner, G.  
330 K.(2010). Contributions of stratospheric water vapor to decadal changes in the rate of global warming.  
331 *Science*, 327: 1219–1223. <https://doi.org/10.1126/science.1182488>

332 Su, H, Read, W, Jiang, J. H. , Waters, J. W. , and Fetzer, E. J. . (2006).Enhanced positive water vapor  
333 feedback associated with tropical deep convection: New evidence from Aura MLS. *Geophys. Res.*  
334 *Lett.* ; 33. <https://doi.org/10.1029/2005GL025505>

335 Stohl, A., Forster, C., Frank, A., et al.: Technical note: The Lagrangian particle dispersion model  
336 FLEXPART version 6.2. *Atmos. Chem. Phys.*, 2005, 5, 2461 – 2474.

337 Tian, B, Soden, B, Wu, X. (2004). Diurnal cycle of convection, clouds, and water vapor in the tropical  
338 upper troposphere: Satellites versus a general circulation model. *J. Geophys. Res. Atmos.*; 27: 2173-  
339 2176. <https://doi.org/10.1029/2003JD004117>

340 Tian, W. S., Chipperfield, M. and Lü, D. R.(2009) .Impact of increasing stratospheric water vapor on ozone  
341 depletion and temperature change. *Adv. Atmos. Sci.* ; 26: 423–437.[https://doi.org/10.1007/s00376-009-](https://doi.org/10.1007/s00376-009-0423-3)  
342 0423-3

343 Wang, Y, Zhang, Y, Chiew, F., McVicar, T., R., Zhang, L., Li, H., and Qin , G. (2017). Contrasting runoff  
344 trends between dry and wet parts of eastern Tibetan Plateau, *Sci. Rep. U.K.* 7: 15458.  
345 <https://doi.org/10.1038/s41598-017-15678-x>

346 Xie, F., Zhou, X. ,Li, J. , Chen, Q. , Zhang, J. , Li, Y.,Ding, R. ,Xue, J. and Ma, X. (2018). Effect of the  
347 Indo-Pacific Warm Pool on lower stratospheric water vapor and comparison with the effect of the El  
348 Niño–Southern Oscillation. *J. Clim.* 31:929–943.

349 Xu, K., Zhong, L., Ma, Y., Zou,M., and Huang Z., (2020). A study on the water vapor transport trend and  
350 water vapor source of the Tibetan Plateau. *Theor. Appl. Climatol.*, **140**, 1031–1042,  
351 <https://doi.org/10.1007/s00704-020-03142-2>.

352 Xu, X, Zhao, T, Lu C., Guo, Y., Chen, B., Liu, R., Li, Y., and Shi, X. (2014).An important mechanism  
353 sustaining the atmospheric "water tower" over the Tibetan Plateau. *Atmos. Chem. Phys.* 14: 11287-  
354 11295.<https://doi.org/10.5194/acp-14-11287-2014>

355 Xu, X., Lu, C. Shi, X. and Gao, S. (2008). World water tower: An atmospheric perspective, *Geophys. Res.*  
356 *Lett.*, 35, L20815. <https://doi.org/10.1029/2008GL035867>

357 Yanai, M. , Esbensen, S. , and Chu, J. H. . (1973). Determination of bulk properties of tropical cloud  
358 clusters from large-scale heat and moisture budgets. *Journal of Atmospheric Sciences*, 30(4), 611-  
359 627.[https://doi.org/10.1175/1520-0469\(1973\)030<0611:DOBPOT>2.0.CO;2](https://doi.org/10.1175/1520-0469(1973)030<0611:DOBPOT>2.0.CO;2)

360

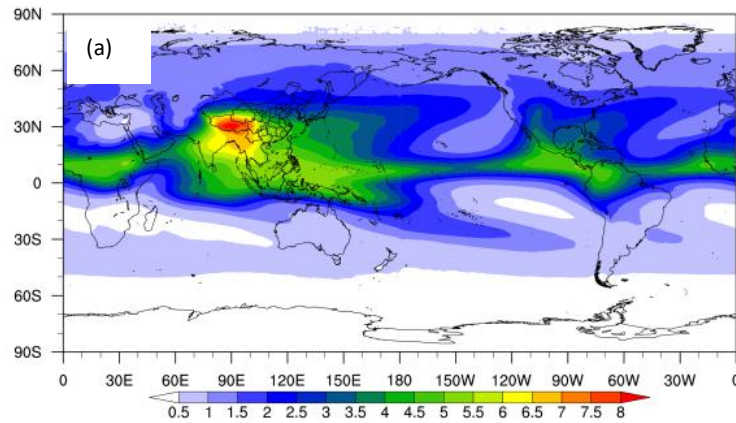
361

362

363

364

365

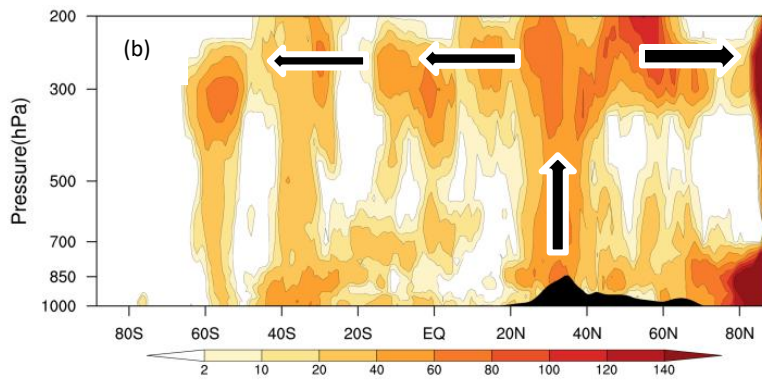


366

367

368

369



370

371 **Figure 1.** (a) The global distribution of the total water vapor from 300 hPa to 500 hPa

372 based on the summertime AIRS data from 2003 to 2018, (b) the vertical section of the

373 frequency (shaded) of the correlation coefficients passing the level of 90%

374 confidence between summertime TP's low cloud cover and the water vapor at different

375 vertical levels along the meridional direction averaged over 60°E - 180°E for 1979-

376 2016 with the black arrows indicating the connections of TP's low clouds to global water

377 vapor in the upper troposphere with high frequencies.

378

379

380

381

382

383

384

385

386

387

388

389

390

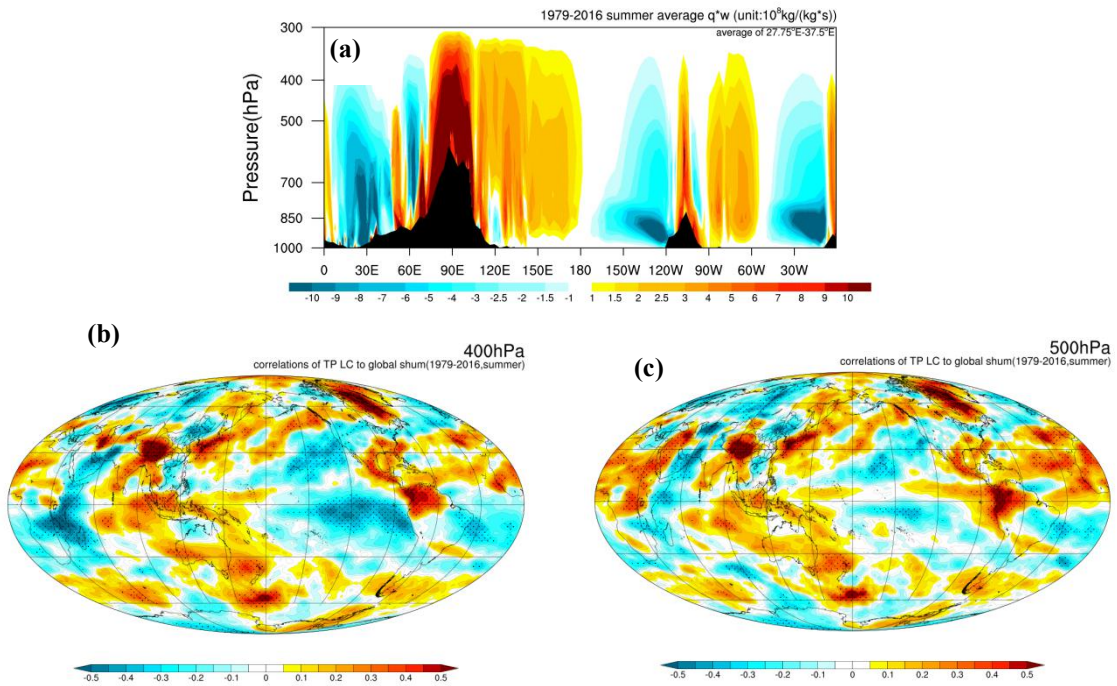
391

392

393

394

395



396 **Figure 2.** (a) The vertical section of vertical vapor transport flux averaged over 27.5-  
397 32.0°N in summers of 1979-2016; the spatial distributions of correlation coefficients of  
398 low cloud cover over the TP with the global specific humidity of the ECMWF-interim  
399 data in Summer (June, July and August) from 1979 to 2018 at (b) 400hPa and (c) 500hPa.

400

401

402

403

404

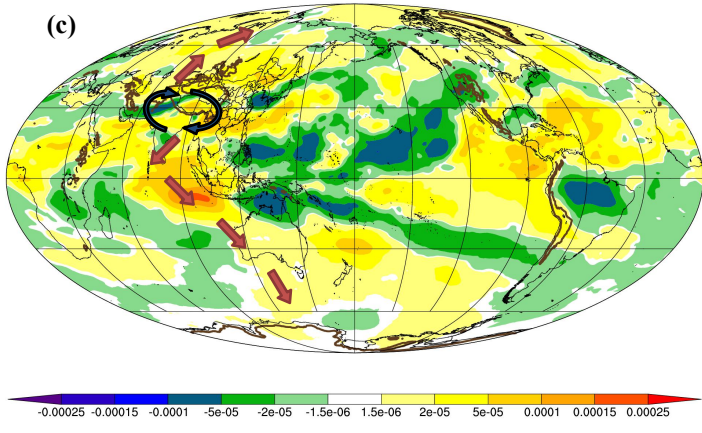
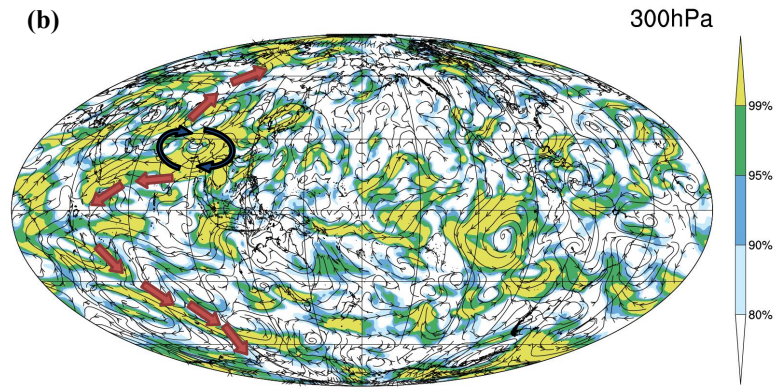
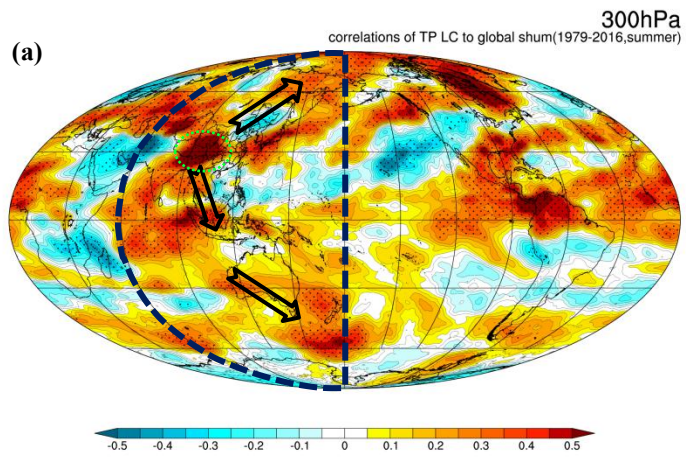
405

406

407

408

409  
410  
411  
412  
413  
414  
415  
416  
417  
418  
419  
420  
421  
422  
423  
424  
425  
426  
427  
428



429

430

431

432

433

434

435

436

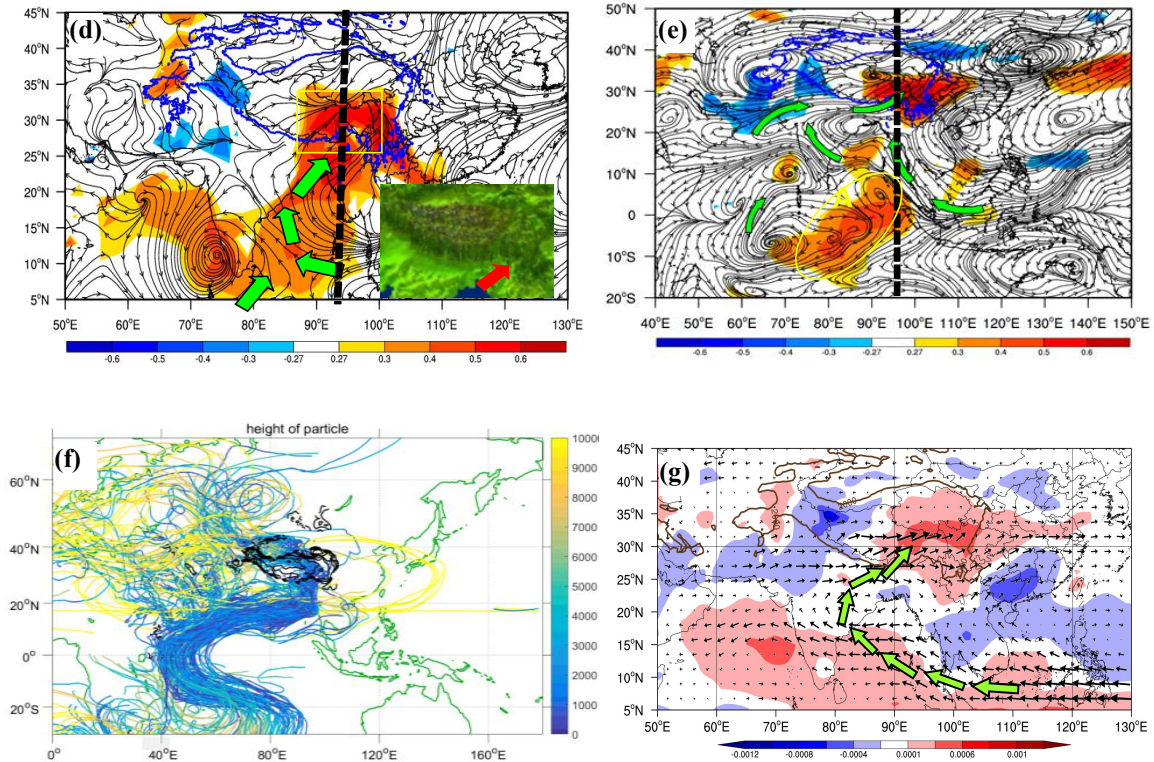
437

438

439

440

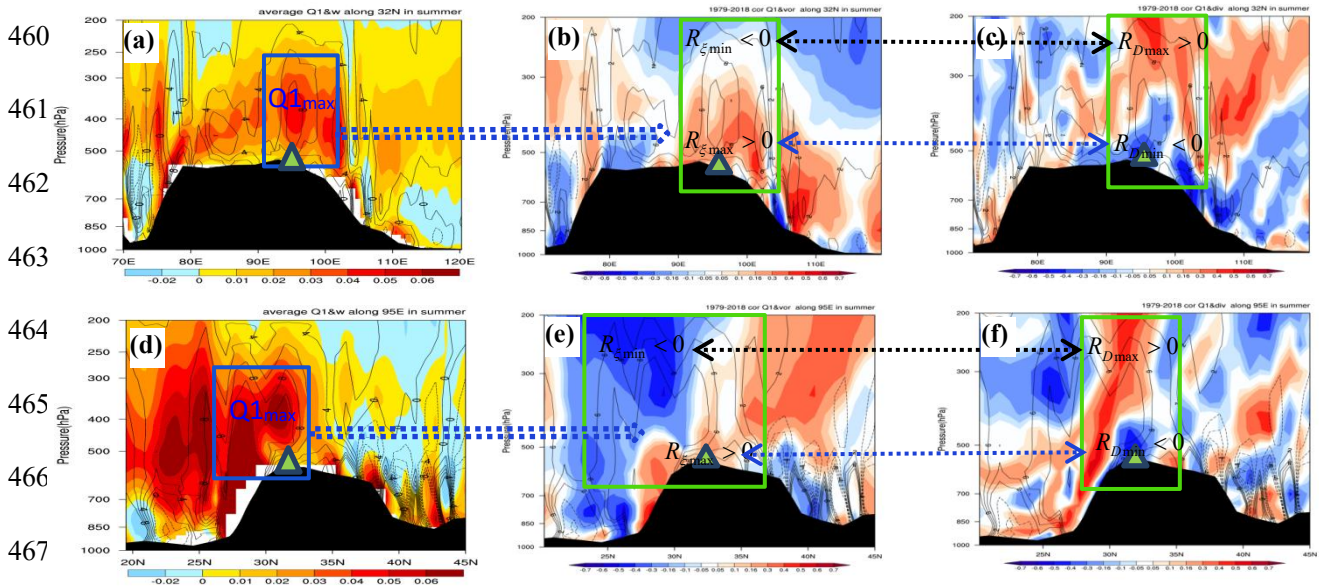
441



442 **Figure 3.** (a) The spatial distributions of correlation coefficients of low cloud cover over the TP  
443 with the global specific humidity of the ECMWF-interim data at 300 hPa in summers of 1979-  
444 2016 with the pathways of convective air to the troposphere; (b) correlation vectors of the column  
445  $Q_1$  integrated vertically over the TP region (80-102°E; 30-37.5°N) with the 300hPa vapor  
446 transport flux in July of 2014-2016, The shaded area indicates the correlation coefficient passing  
447 the the 90% confidence level; (c) the difference of specific humidity (shading, unit:kg/kg) at 300  
448 hPa in summer in 1998 and 2007 with anomalously high  $Q_1$  and in 1997 and 2003 with  
449 anomalously low  $Q_1$  in the AWT, The black and orange arrows indicate respectively the  
450 anticyclonic circulations in the TP and water vapor transport pathways from the TP to the Arctic  
451 and Antarctic regions.; the correlation field between the total apparent heat source  $Q_1$  over the TP  
452 region (80-102°E; 30-37.5°N) with the water vapor (shaded) and water vapor flux (stream lines)

453 in the surface layer (d) and middle layer (500hpa) (e) in summer over 1979-2015, respectively, (f)  
 454 the backward trajectories of water vapor transport simulated with the model FLEXPART in July,  
 455 2009. (g) the difference of vapor transport flux at 500 hPa (vectors, unit:gs<sup>-1</sup>hPa<sup>-1</sup>cm<sup>-1</sup>) and  
 456 specific humidity (color contours, unit:kg/kg) between summers with anomalously high Q<sub>1</sub> in  
 457 1998, 2005, 2007, 2008 and 2009 and with anomalously low Q<sub>1</sub> in 1994, 1997, 2001, 2002 and  
 458 2003 over the TP

459



468

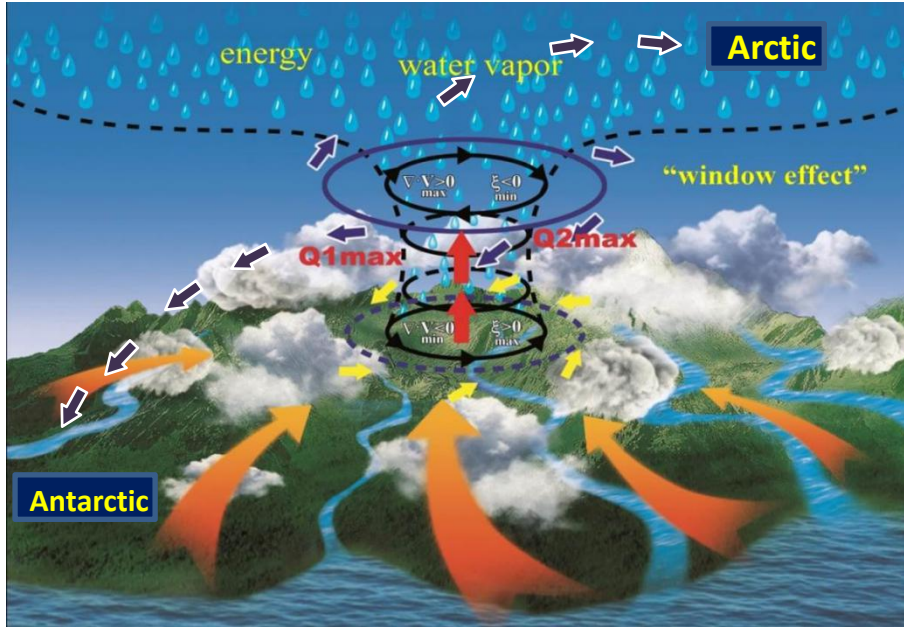
469 **Figure 4.**The vertical sections of (a,d) vertical motion (contours, in unit: 10<sup>-2</sup>Pa·s<sup>-1</sup>) and column  
 470 Q<sub>1</sub> (color contours, in unit:10<sup>-3</sup>w kg<sup>-1</sup>) ; (b,e) vertical motion (contours, in unit: 10<sup>-2</sup>Pa·s<sup>-1</sup>) and  
 471 correlation coefficients (color contours) between Q<sub>1</sub> and the vorticity as well as (c,f) vertical  
 472 motion (contours, in unit: 10<sup>-2</sup>Pa·s<sup>-1</sup>) and the correlation coefficients between Q<sub>1</sub> and the  
 473 divergence (contours) in the TP, with Figs. a, b and c along 32 °N, and Figs. d, e and f along 95  
 474 °E. The green triangles indicate the AWT core region.

475

476

477

478



479

480 **Figure 5.** A diagram of vertical water vapor transport in the troposphere driven by the  
481 thermal forcing of AWT over the TP, where the vertical transport window of water vapor  
482 in the troposphere connects globally the water vapor transport from the tropical oceans  
483 and the southern Indian Ocean in the lower troposphere with transport to the Arctic and  
484 Antarctic regions in the upper troposphere.

485

486

487